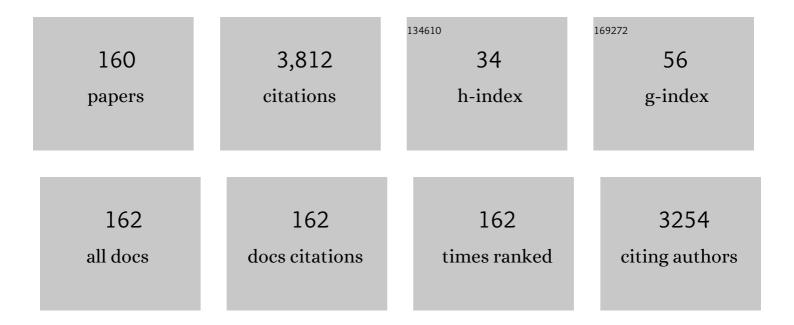
## Meng-Xing Tang

List of Publications by Year in descending order

Source: https://exaly.com/author-pdf/1286381/publications.pdf Version: 2024-02-01



#	Article	IF	CITATIONS
1	Spatial Response Identification Enables Robust Experimental Ultrasound Computed Tomography. IEEE Transactions on Ultrasonics, Ferroelectrics, and Frequency Control, 2022, 69, 27-37.	1.7	9
2	Acoustic Beam Mapping for Guiding HIFU Therapy In Vivo Using Sub-Therapeutic Sound Pulse and Passive Beamforming. IEEE Transactions on Biomedical Engineering, 2022, 69, 1663-1673.	2.5	5
3	Ultrafast 3-D Ultrasound Imaging Using Row–Column Array-Specific Frame-Multiply-and-Sum Beamforming. IEEE Transactions on Ultrasonics, Ferroelectrics, and Frequency Control, 2022, 69, 480-488.	1.7	14
4	Evaluation of contrast enhancement ultrasound images of Sonazoid microbubbles in tissue-mimicking phantom obtained by optimal Golay pulse compression. Japanese Journal of Applied Physics, 2022, 61, SG1015.	0.8	3
5	Contrast Agent-Free Assessment of Blood Flow and Wall Shear Stress in the Rabbit Aorta using Ultrasound Image Velocimetry. Ultrasound in Medicine and Biology, 2022, 48, 437-449.	0.7	7
6	Stride: A flexible software platform for high-performance ultrasound computed tomography. Computer Methods and Programs in Biomedicine, 2022, 221, 106855.	2.6	9
7	Imaging With Therapeutic Acoustic Wavelets–Short Pulses Enable Acoustic Localization When Time of Arrival is Combined With Delay and Sum. IEEE Transactions on Ultrasonics, Ferroelectrics, and Frequency Control, 2021, 68, 178-190.	1.7	8
8	Spatial Response Identification for Flexible and Accurate Ultrasound Transducer Calibration and its Application to Brain Imaging. IEEE Transactions on Ultrasonics, Ferroelectrics, and Frequency Control, 2021, 68, 143-153.	1.7	5
9	Volumetric Flow Estimation in a Coronary Artery Phantom Using High-Frame-Rate Contrast-Enhanced Ultrasound, Speckle Decorrelation, and Doppler Flow Direction Detection. IEEE Transactions on Ultrasonics, Ferroelectrics, and Frequency Control, 2021, 68, 3299-3308.	1.7	2
10	Selection on Golay complementary sequences in binary pulse compression for microbubble detection. Japanese Journal of Applied Physics, 2021, 60, 066501.	0.8	3
11	A kit-based aluminium-[ <sup>18</sup> F]fluoride approach to radiolabelled microbubbles. Chemical Communications, 2021, 57, 11677-11680.	2.2	3
12	4D ultrafast blood flow imaging comparison: vector Doppler, transverse oscillation and speckle tracking. , 2021, , .		0
13	Effects of Aberration on Super-Resolution Ultrasound Imaging using Microbubbles. , 2021, , .		0
14	Volumetric Super-Resolution Ultrasound with a 1D array probe: a simulation study. , 2021, , .		0
15	Investigating CXCR4 expression of tumor cells and the vascular compartment: A multimodal approach. PLoS ONE, 2021, 16, e0260186.	1.1	1
16	Wave Intensity Analysis Combined With Machine Learning can Detect Impaired Stroke Volume in Simulations of Heart Failure. Frontiers in Bioengineering and Biotechnology, 2021, 9, 737055.	2.0	2
17	3-D Super-Resolution Ultrasound Imaging With a 2-D Sparse Array. IEEE Transactions on Ultrasonics, Ferroelectrics, and Frequency Control, 2020, 67, 269-277.	1.7	74
18	Comparison of arterial wave intensity analysis by pressure–velocity and diameter–velocity methods in a virtual population of adult subjects. Proceedings of the Institution of Mechanical Engineers, Part H: Journal of Engineering in Medicine, 2020, 234, 1260-1276.	1.0	6

#	Article	IF	CITATIONS
19	Doppler Passive Acoustic Mapping. IEEE Transactions on Ultrasonics, Ferroelectrics, and Frequency Control, 2020, 67, 2692-2703.	1.7	3
20	Contrast-Enhanced High-Frame-Rate Ultrasound Imaging of Flow Patterns in Cardiac Chambers and Deep Vessels. Ultrasound in Medicine and Biology, 2020, 46, 2875-2890.	0.7	15
21	Effects of Mechanical Index on Repeated Sparse Activation of Nanodroplets In Vivo. , 2020, , .		1
22	Determining Haemodynamic Wall Shear Stress in the Rabbit Aorta In Vivo Using Contrast-Enhanced Ultrasound Image Velocimetry. Annals of Biomedical Engineering, 2020, 48, 1728-1739.	1.3	15
23	Full-waveform inversion imaging of the human brain. Npj Digital Medicine, 2020, 3, 28.	5.7	108
24	Clinical quantitative cardiac imaging for the assessment of myocardial ischaemia. Nature Reviews Cardiology, 2020, 17, 427-450.	6.1	94
25	Super-resolution Ultrasound Imaging. Ultrasound in Medicine and Biology, 2020, 46, 865-891.	0.7	253
26	Quantitative Microvessel Analysis with 3-D Super-Resolution Ultrasound and Velocity Mapping. , 2020, , .		5
27	3D super localized flow with locally and acoustically activated nanodroplets and high frame rate imaging using a matrix array. , 2020, , .		1
28	Localization of a Scatterer in 3D with a Single Measurement and Single Element Transducer. , 2020, , .		1
29	Measurement of Flow Volume in the Presence of Reverse Flow with Ultrasound Speckle Decorrelation. Ultrasound in Medicine and Biology, 2019, 45, 3056-3066.	0.7	7
30	Optimization of 3-D Divergence-Free Flow Field Reconstruction Using 2-D Ultrasound Vector Flow Imaging. Ultrasound in Medicine and Biology, 2019, 45, 3042-3055.	0.7	3
31	Poisson Statistical Model of Ultrasound Super-Resolution Imaging Acquisition Time. IEEE Transactions on Ultrasonics, Ferroelectrics, and Frequency Control, 2019, 66, 1246-1254.	1.7	40
32	High Frame Rate Contrast-Enhanced Ultrasound Imaging for Slow Lymphatic Flow: Influence of Ultrasound Pressure and Flow Rate on Bubble Disruption and Image Persistence. Ultrasound in Medicine and Biology, 2019, 45, 2456-2470.	0.7	9
33	3-D Flow Reconstruction Using Divergence-Free Interpolation of Multiple 2-D Contrast-Enhanced Ultrasound Particle Imaging Velocimetry Measurements. Ultrasound in Medicine and Biology, 2019, 45, 795-810.	0.7	14
34	Investigation of Microbubble Detection Methods for Super-Resolution Imaging of Microvasculature. IEEE Transactions on Ultrasonics, Ferroelectrics, and Frequency Control, 2019, 66, 676-691.	1.7	29
35	Developing and using fast shear wave elastography to quantify physiologically-relevant tendon forces. Medical Engineering and Physics, 2019, 69, 116-122.	0.8	11
36	Development of <sup>68</sup> Ga-labelled ultrasound microbubbles for whole-body PET imaging. Chemical Science, 2019, 10, 5603-5615.	3.7	13

#	Article	IF	CITATIONS
37	Fast Acoustic Wave Sparsely Activated Localization Microscopy: Ultrasound Super-Resolution Using Plane-Wave Activation of Nanodroplets. IEEE Transactions on Ultrasonics, Ferroelectrics, and Frequency Control, 2019, 66, 1039-1046.	1.7	53
38	3D Super-Resolution US Imaging of Rabbit Lymph Node Vasculature in Vivo by Using Microbubbles. Radiology, 2019, 291, 642-650.	3.6	82
39	3-D Microvascular Imaging Using High Frame Rate Ultrasound and ASAP Without Contrast Agents: Development and Initial <i>In Vivo</i> Evaluation on Nontumor and Tumor Models. IEEE Transactions on Ultrasonics, Ferroelectrics, and Frequency Control, 2019, 66, 939-948.	1.7	11
40	Quantification of Vaporised Targeted Nanodroplets Using High-Frame-Rate Ultrasound and Optics. Ultrasound in Medicine and Biology, 2019, 45, 1131-1142.	0.7	12
41	Diagnosing and Managing the Malignant Axilla in Breast Cancer. Current Breast Cancer Reports, 2019, 11, 1-8.	0.5	2
42	Contrast-Enhanced Photoacoustic Imaging of Low-boiling-point Phase-Change Nanodroplets. , 2019, , .		7
43	High Signal-to-Noise Ratio Contrast-Enhanced Photoacoustic Imaging using Acoustic Sub-Aperture Processing and Spatiotemporal Filtering. , 2019, , .		8
44	Sparse Image Reconstruction for Contrast Enhanced Cardiac Ultrasound using Diverging Waves. , 2019, , .		0
45	Super-Resolution Ultrasound Image Filtering with Machine-Learning to Reduce the Localization Error. , 2019, , .		4
46	Photoacoustic Super-Resolution Imaging using Laser Activation of Low-Boiling-Point Dye-Coated Nanodroplets in vitro and in vivo. , 2019, , .		5
47	Minimization of Nanodroplet Activation Time using Focused-Pulses for Droplet-Based Ultrasound Super-Resolution Imaging. , 2019, , .		5
48	Activation and 3D Imaging of Phase-change Nanodroplet Contrast Agents with a 2D Ultrasound Probe. , 2019, , .		2
49	Acoustic Wave Sparsely-Activated Localization Microscopy (AWSALM): In Vivo Fast Ultrasound Super-Resolution Imaging using Nanodroplets. , 2019, , .		9
50	Motion Artifacts and Correction in Multipulse High-Frame Rate Contrast-Enhanced Ultrasound. IEEE Transactions on Ultrasonics, Ferroelectrics, and Frequency Control, 2019, 66, 417-420.	1.7	12
51	Enhanced pre-operative axillary staging using intradermal microbubbles and contrast-enhanced ultrasound to detect and biopsy sentinel lymph nodes in breast cancer: a potential replacement for axillary surgery. British Journal of Radiology, 2018, 91, 20170626.	1.0	19
52	Imaging of vaporised sub-micron phase change contrast agents with high frame rate ultrasound and optics. Physics in Medicine and Biology, 2018, 63, 065002.	1.6	21
53	Fully Automatic Myocardial Segmentation of Contrast Echocardiography Sequence Using Random Forests Guided by Shape Model. IEEE Transactions on Medical Imaging, 2018, 37, 1081-1091.	5.4	38
54	High Frame-Rate Contrast Echocardiography: In-Human Demonstration. JACC: Cardiovascular Imaging, 2018, 11, 923-924.	2.3	29

#	Article	IF	CITATIONS
55	Two-Stage Motion Correction for Super-Resolution Ultrasound Imaging in Human Lower Limb. IEEE Transactions on Ultrasonics, Ferroelectrics, and Frequency Control, 2018, 65, 803-814.	1.7	89
56	ASAP: Super-Contrast Vasculature Imaging Using Coherence Analysis and High Frame-Rate Contrast Enhanced Ultrasound. IEEE Transactions on Medical Imaging, 2018, 37, 1847-1856.	5.4	35
57	Spatio-Temporal Flow and Wall Shear Stress Mapping Based on Incoherent Ensemble-Correlation of Ultrafast Contrast Enhanced Ultrasound Images. Ultrasound in Medicine and Biology, 2018, 44, 134-152.	0.7	57
58	3-D Motion Correction for Volumetric Super-Resolution Ultrasound Imaging. , 2018, 2018, .		8
59	Contrast vs Non-Contrast Enhanced Microvascular Imaging Using Acoustic Sub-Aperture Processing (ASAP): In Vivo Demonstration. , 2018, , .		1
60	3D in Vitro Ultrasound Super-Resolution Imaging Using a Clinical System. , 2018, , .		5
61	Flow Visualization Through Locally Activated Nanodroplets and High Frame Rate Imaging. , 2018, , .		7
62	High-Contrast 3D in Vivo Microvascular Imaging Using Scanning 2D Ultrasound and Acoutic Sub-Aperture Processing (ASAP). , 2018, , .		1
63	Investigation of Nanodroplet Adhesion to Endothelial Cells Under Atheroprone Flow Conditions. , 2018, , .		5
64	Introduction to the Special Issue on High Frame Rate/Ultrafast Contrast-Enhanced Ultrasound Imaging. IEEE Transactions on Ultrasonics, Ferroelectrics, and Frequency Control, 2018, 65, 2210-2211.	1.7	2
65	Fast Acoustic Wave Sparsely Activated Localization Microscopy (Fast-AWSALM) Using Octafluoropropane N Anodroplets. , 2018, , .		4
66	3D Flow Reconstruction and Wall Shear Stress Evaluation with 2D Ultrafast Ultrasound Particle Imaging Velocimetry. , 2018, , .		0
67	High-Frame-Rate Contrast Echocardiography Using Diverging Waves: Initial <i>In Vitro</i> and <i>In Vivo</i> Evaluation. IEEE Transactions on Ultrasonics, Ferroelectrics, and Frequency Control, 2018, 65, 2212-2221.	1.7	12
68	3-D Velocity and Volume Flow Measurement \$In~Vivo\$ Using Speckle Decorrelation and 2-D High-Frame-Rate Contrast-Enhanced Ultrasound. IEEE Transactions on Ultrasonics, Ferroelectrics, and Frequency Control, 2018, 65, 2233-2244.	1.7	19
69	Acoustic wave sparsely activated localization microscopy (AWSALM): Super-resolution ultrasound imaging using acoustic activation and deactivation of nanodroplets. Applied Physics Letters, 2018, 113, .	1.5	59
70	10.1063/1.5029874.1., 2018, , .		0
71	Differential Intensity Projection for Visualisation and Quantification of Plaque Neovascularisation in Contrast-Enhanced Ultrasound Images of Carotid Arteries. Ultrasound in Medicine and Biology, 2017, 43, 831-837.	0.7	5
72	Ultrasound imaging velocimetry with interleaved images for improved pulsatile arterial flow measurements: a new correction method, experimental and <i>in vivo</i> validation. Journal of the Royal Society Interface, 2017, 14, 20160761.	1.5	14

#	Article	IF	CITATIONS
73	Optically and acoustically triggerable sub-micron phase-change contrast agents for enhanced photoacoustic and ultrasound imaging. Photoacoustics, 2017, 6, 26-36.	4.4	44
74	Microbubble Axial Localization Errors in Ultrasound Super-Resolution Imaging. IEEE Transactions on Ultrasonics, Ferroelectrics, and Frequency Control, 2017, 64, 1644-1654.	1.7	70
75	Unveiling the development of intracranial injury using dynamic brain EIT: an evaluation of current reconstruction algorithms. Physiological Measurement, 2017, 38, 1776-1790.	1.2	24
76	Reproducible Computer-Assisted Quantification of Myocardial Perfusion with Contrast-Enhanced Ultrasound. Ultrasound in Medicine and Biology, 2017, 43, 2235-2246.	0.7	4
77	Effects of microchannel confinement on acoustic vaporisation of ultrasound phase change contrast agents. Physics in Medicine and Biology, 2017, 62, 6884-6898.	1.6	29
78	A Temporal and Spatial Analysis Approach to Automated Segmentation of Microbubble Signals in Contrast-Enhanced Ultrasound Images: Application to Quantification of Active Vascular Density in Human Lower Limbs. Ultrasound in Medicine and Biology, 2017, 43, 2221-2234.	0.7	0
79	3-D <i>In Vitro</i> Acoustic Super-Resolution and Super-Resolved Velocity Mapping Using Microbubbles. IEEE Transactions on Ultrasonics, Ferroelectrics, and Frequency Control, 2017, 64, 1478-1486.	1.7	48
80	Notice of Removal: 3D flow velocity reconstruction in a human radial artery from measured 2D high-frame-rate plane wave contrast enhanced ultrasound in two scanning directions — A feasibility study. , 2017, , .		0
81	Two Stage Sub-Wavelength Motion Correction in Human Microvasculature for CEUS Imaging. , 2017, , .		5
82	Acoustic response of targeted nanodroplets post-activation using high frame rate imaging. , 2017, , .		9
83	Localisation of multiple non-isolated microbubbles with frequency decomposition in super-resolution imaging. , 2017, , .		1
84	High frame rate contrast enhanced echocardiography: Microbubbles stability and contrast evaluation. , 2017, , .		0
85	Investigation of microbubble detection methods for super-resolution imaging of microvasculature. , 2017, , .		1
86	Multi-frame rate plane wave contrast-enhanced ultrasound imaging for tumour vascular imaging and perfusion quantification. , 2017, , .		2
87	Two stage sub-wavelength motion correction in human microvasculature for CEUS imaging. , 2017, , .		6
88	Effects of motion on high frame rate contrast enhanced echocardiography and its correction. , 2017, ,		0
89	Acoustic response of phase change contrast agents targeted with breast cancer cells immediately after ultrasonic activation using ultrafast imaging. , 2017, , .		0
90	Multi-frame rate plane wave contrast-enhance ultrasound imaging for tumour vasculature imaging and perfusion quantification. , 2017, , .		0

#	Article	IF	CITATIONS
91	Ultrasound super-resolution with microbubble contrast agents. , 2017, , .		0
92	Cardiac flow mapping using high frame-rate diverging wave contrast enhanced ultrasound and image tracking. , 2017, , .		0
93	Cardiac flow mapping using high frame rate diverging wave contrast enhanced ultrasound and image tracking. , 2017, , .		1
94	Notice of Removal: Optically and acoustically triggerable sub-micron phase-change contrast agents for enhanced photoacoustic and ultrasound imaging. , 2017, , .		0
95	High frame rate contrast enhanced echocardiography: Microbubbles stability and contrast evaluation. , 2017, , .		4
96	Notice of Removal: Exploring mild bubble disruption and high frame rate contrast enhanced ultrasound for specific imaging of lymphatic vessel. , 2017, , .		0
97	High frame rate ultrasound imaging of vaporised phase change contrast agents. , 2017, , .		4
98	High frame rate ultrasound imaging of vaporised sub-micron phase-change contrast agents. , 2017, , .		0
99	Single transducer LOVIT-enabled photoacoustic imaging: A feasibility study. , 2016, , .		1
100	Rapid short-pulse sequences enhance the spatiotemporal uniformity of acoustically driven microbubble activity during flow conditions. Journal of the Acoustical Society of America, 2016, 140, 2469-2480.	0.5	37
101	Contrast enhancement of carotid adventitial vasa vasorum as a biomarker of radiation-induced atherosclerosis. Radiotherapy and Oncology, 2016, 120, 63-68.	0.3	7
102	Automated segmentation of blood vessel in contrast enhanced plane wave ultrasound images. , 2016, , .		0
103	Vaporising phase change ultrasound contrast agent in microvascular confinement. , 2016, , .		10
104	Ultrasound Imaging with Microbubbles [Life Sciences]. IEEE Signal Processing Magazine, 2016, 33, 111-117.	4.6	21
105	10.1121/1.4964271.1.,2016,,.		0
106	Super-resolution imaging of microbubble contrast agents. , 2015, , .		0
107	A Targeting Microbubble for Ultrasound Molecular Imaging. PLoS ONE, 2015, 10, e0129681.	1.1	38
108	Correction of Non-Linear Propagation Artifact in Contrast-Enhanced Ultrasound Imaging of Carotid Arteries: Methods and inÂVitro Evaluation. Ultrasound in Medicine and Biology, 2015, 41, 1938-1947.	0.7	18

#	Article	IF	CITATIONS
109	Quantitative Ultrasound Molecular Imaging. Ultrasound in Medicine and Biology, 2015, 41, 2478-2496.	0.7	12
110	Motion correction in contrast-enhanced ultrasound scans of carotid atherosclerotic plaques. , 2015, , .		0
111	Quantifying Activation of Perfluorocarbon-Based Phase-Change Contrast Agents Using Simultaneous Acoustic and Optical Observation. Ultrasound in Medicine and Biology, 2015, 41, 1422-1431.	0.7	26
112	Attenuation Correction and Normalisation for Quantification of Contrast Enhancement in Ultrasound Images of Carotid Arteries. Ultrasound in Medicine and Biology, 2015, 41, 1876-1883.	0.7	10
113	Decompression induced bubble dynamics on ex vivo fat and muscle tissue surfaces with a new experimental set up. Colloids and Surfaces B: Biointerfaces, 2015, 129, 121-129.	2.5	13
114	Detecting tissue optical and mechanical properties with an ultrasound modulated optical imaging system in reflection detection geometry. Biomedical Optics Express, 2015, 6, 63.	1.5	6
115	Dual shear wave induced laser speckle contrast signal and the improvement in shear wave speed measurement. Biomedical Optics Express, 2015, 6, 1954.	1.5	4
116	Flow Velocity Mapping Using Contrast Enhanced High-Frame-Rate Plane Wave Ultrasound and Image Tracking: Methods and Initial inÂVitro and inÂVivo Evaluation. Ultrasound in Medicine and Biology, 2015, 41, 2913-2925.	0.7	147
117	Surface Charge Measurement of SonoVue, Definity and Optison: A Comparison of Laser Doppler Electrophoresis and Micro-Electrophoresis. Ultrasound in Medicine and Biology, 2015, 41, 2990-3000.	0.7	24
118	Microbubble Void Imaging: A Non-invasive Technique for Flow Visualisation and Quantification of Mixing in Large Vessels Using Plane Wave Ultrasound and Controlled Microbubble Contrast Agent Destruction. Ultrasound in Medicine and Biology, 2015, 41, 2926-2937.	0.7	19
119	In Vivo Acoustic Super-Resolution and Super-Resolved Velocity Mapping Using Microbubbles. IEEE Transactions on Medical Imaging, 2015, 34, 433-440.	5.4	315
120	Tracking shear waves in turbid medium by light: theory, simulation, and experiment. Optics Letters, 2014, 39, 1597.	1.7	7
121	Circulatory bubble dynamics: From physical to biological aspects. Advances in Colloid and Interface Science, 2014, 206, 239-249.	7.0	55
122	Dynamics of Targeted Microbubble Adhesion Under Pulsatile Compared with Steady Flow. Ultrasound in Medicine and Biology, 2014, 40, 2445-2457.	0.7	1
123	Emerging Imaging Technologies in Medicine. Ultrasound in Medicine and Biology, 2014, 40, 2542.	0.7	0
124	Use of Electrical Impedance Tomography to Monitor Regional Cerebral Edema during Clinical Dehydration Treatment. PLoS ONE, 2014, 9, e113202.	1.1	50
125	The use of portable 2D echocardiography and 'frame-based' bubble counting as a tool to evaluate diving decompression stress. Diving and Hyperbaric Medicine, 2014, 44, 5-13.	0.2	15
126	Single Bubble Acoustic Characterization and Stability Measurement of Adherent Microbubbles. Ultrasound in Medicine and Biology, 2013, 39, 903-914.	0.7	10

#	Article	IF	CITATIONS
127	Viscosity measurement based on shear-wave laser speckle contrast analysis. Journal of Biomedical Optics, 2013, 18, 121511.	1.4	6
128	Ultrasound Imaging Velocimetry: Effect of Beam Sweeping on Velocity Estimation. Ultrasound in Medicine and Biology, 2013, 39, 1672-1681.	0.7	26
129	Acoustic super-resolution with ultrasound and microbubbles. Physics in Medicine and Biology, 2013, 58, 6447-6458.	1.6	225
130	Mapping microbubble viscosity using fluorescence lifetime imaging of molecular rotors. Proceedings of the National Academy of Sciences of the United States of America, 2013, 110, 9225-9230.	3.3	128
131	Evaluation of Methods for Sizing and Counting of Ultrasound Contrast Agents. Ultrasound in Medicine and Biology, 2012, 38, 834-845.	0.7	42
132	Theoretical and Experimental Characterisation of Magnetic Microbubbles. Ultrasound in Medicine and Biology, 2012, 38, 864-875.	0.7	32
133	The Influence of Gas Saturation on Microbubble Stability. Ultrasound in Medicine and Biology, 2012, 38, 1097-1100.	0.7	26
134	Effect of Albumin and Dextrose Concentration on Ultrasound and Microbubble Mediated Gene Transfection InÂVivo. Ultrasound in Medicine and Biology, 2012, 38, 1067-1077.	0.7	14
135	Shear Wave Elasticity Imaging Based on Acoustic Radiation Force and Optical Detection. Ultrasound in Medicine and Biology, 2012, 38, 1637-1645.	0.7	19
136	Effect of ultrasound on adherent microbubble contrast agents. Physics in Medicine and Biology, 2012, 57, 6999-7014.	1.6	6
137	Modeling non-spherical oscillations and stability of acoustically driven shelled microbubbles. Journal of the Acoustical Society of America, 2012, 131, 4349-4357.	0.5	8
138	Understanding the Structure and Mechanism of Formation of a New Magnetic Microbubble Formulation. Theranostics, 2012, 2, 1127-1139.	4.6	18
139	Effects of acoustic radiation force and shear waves for absorption and stiffness sensing in ultrasound modulated optical tomography. Optics Express, 2011, 19, 7299.	1.7	23
140	Effect of bubble shell nonlinearity on ultrasound nonlinear propagation through microbubble populations. Journal of the Acoustical Society of America, 2011, 129, EL76-EL82.	0.5	16
141	Temperature-Dependent Differences in the Nonlinear Acoustic Behavior of Ultrasound Contrast Agents Revealed by High-Speed Imaging and Bulk Acoustics. Ultrasound in Medicine and Biology, 2011, 37, 1509-1517.	0.7	26
142	Performance Evaluation of Five Types of Ag/AgCl Bio-Electrodes for Cerebral Electrical Impedance Tomography. Annals of Biomedical Engineering, 2011, 39, 2059-2067.	1.3	42
143	Influence of Needle Gauge On In Vivo Ultrasound and Microbubble-Mediated Gene Transfection. Ultrasound in Medicine and Biology, 2011, 37, 1531-1537.	0.7	19
144	Ultrasound-mediated optical tomography: a review of current methods. Interface Focus, 2011, 1, 632-648.	1.5	67

#	Article	IF	CITATIONS
145	Effects of Nonlinear Propagation in Ultrasound Contrast Agent Imaging. Ultrasound in Medicine and Biology, 2010, 36, 459-466.	0.7	64
146	On Sizing and Counting of Microbubbles Using Optical Microscopy. Ultrasound in Medicine and Biology, 2010, 36, 2093-2096.	0.7	66
147	Parallel detection of amplitude-modulated, ultrasound-modulated optical signals. Optics Letters, 2010, 35, 2633.	1.7	10
148	Enhanced gene transfection in vivo using magnetic localisation of ultrasound contrast agents: Preliminary results. , 2010, , .		8
149	Verification of an image calibration method in ultrasound contrast agent imaging on a perfusion phantom. , 2009, , .		Ο
150	Ultrasound phase velocities in SonoVue <sup>™</sup> as a function of pressure and bubble concentration. , 2009, , .		5
151	Attenuation Correction in Ultrasound Contrast Agent Imaging: Elementary Theory and Preliminary Experimental Evaluation. Ultrasound in Medicine and Biology, 2008, 34, 1998-2008.	0.7	28
152	Frequency and pressure dependent attenuation and scattering by microbubbles. Ultrasound in Medicine and Biology, 2007, 33, 164-168.	0.7	72
153	Microbubble Contrast Agent Detection Using Binary Coded Pulses. Ultrasound in Medicine and Biology, 2007, 33, 1787-1795.	0.7	20
154	Nonlinear propagation of ultrasound through microbubble contrast agents and implications for imaging. IEEE Transactions on Ultrasonics, Ferroelectrics, and Frequency Control, 2006, 53, 2406-2415.	1.7	78
155	Pressure-dependent attenuation with microbubbles at low mechanical index. Ultrasound in Medicine and Biology, 2005, 31, 377-384.	0.7	51
156	Exact Confidence Interval for Magnitude-Squared Coherence Estimates. IEEE Signal Processing Letters, 2004, 11, 326-329.	2.1	42
157	The number of electrodes and basis functions in EIT image reconstruction. Physiological Measurement, 2002, 23, 129-140.	1.2	60
158	A comparison of methods for measurement of spatial resolution in two-dimensional circular EIT images. Physiological Measurement, 2002, 23, 169-176.	1.2	39
159	Effects of incompatible boundary information in EIT on the convergence behavior of an iterative algorithm. IEEE Transactions on Medical Imaging, 2002, 21, 620-628.	5.4	12
160	Nonlinear corruption of ultasound transmission by microbubble contrast agents. , 0, , .		1